

Landing in Binary Asteroids: A Global Map of Feasible Descent Opportunities for Unpowered Spacecraft

J.P. Sánchez^{a*}, O. Celik^b

^a *Space Research Group, Centre of Autonomous and Cyber-Physical Systems, Cranfield University, UK.*

jp.sanchez@cranfield.ac.uk

^b *Department of Space and Astronautical Sciences, The Graduate University for Advanced Studies (SOKENDAI), Sagami-hara, Japan. onur.celik@ac.jaxa.jp.*

* Corresponding Author

Abstract

Asteroid surface science provides the necessary “ground-truth” to validate and enhance remote sensing from orbiting spacecraft. Yet, due to uncertainties associated with the dynamical environment near asteroids, it is generally prudent for the main spacecraft to remain at a safe distance. Instead, small landers could be used much more daringly. This paper explores the potential for ballistic landing opportunities in binary asteroid systems. The dynamics near a binary asteroid are modelled by means of the Circular Restricted Three Body Problem, which provides a reasonable representation of a standard binary system. Natural landing trajectories are sought that allow for deployment from safe distances and touchdown with minimum local-vertical velocity. The necessary coefficient of restitution to ensure a successful landing and the effects of navigation and deployment errors are also analysed. Assuming deployment errors in the order of 10 meters and 1 cm/s (1-sigma), the results show that ballistic descent landing operations are likely to be successful if targeting near equatorial regions with longitude within 320° to 20° in the secondary of the binary system.

Keywords: Binary asteroid missions, trajectory design, ballistic descent trajectories, circular restricted three body problem, deployment errors and covariance matrix.

1. Introduction

Near Earth asteroids (NEAs) are the easiest celestial objects to reach from Earth (excl. the Moon), and offer a unique window to the early stages of accretion and differentiation of the inner planets of our Solar System. As such, they have become appealing targets for science missions. For such missions, on-board remote sensing instrumentation is paramount, however, in-situ measurements provide the necessary “ground-truth” to enhance the science return.

The chaoticity of the strongly irregular dynamical environment found at asteroids, however, entails some daring challenges for navigation, and thus, most missions spend long periods of times (~months) stationed well beyond the asteroid’s Hill radius, where the heliocentric dynamical environment is still predominant, and thus much more easily predicted.

NanoSats and other shoebox-sized landers have already been identified as potential valuable assets for in-situ asteroid exploration, since, due to their low cost, they can be used much more daringly. However, due to constraints in mass and volume, these systems may only allow for extremely crude orbit and landing control. This paper thus explores the potential for passive landing opportunities that may be enabled by the asteroid’s natural dynamics.

Particularly, the paper focuses on binary asteroid systems, i.e. asteroids with a satellite, which are believed to account for about 15% of the NEA

population. The dynamics near a binary asteroid are then modelled by means of the Circular Restricted Three Body Problem, which provides a reasonably representative model for a standard binary system. Natural landing trajectories are sought that allow for a deployment well outside the orbit of the asteroid’s satellite, and a touchdown with minimum local-vertical velocity.

By taking a purely deterministic approach, the paper provides a global map of the minimum touchdown velocity, as well as the required coefficient of restitution (i.e. energy damping) in order to ensure that the spacecraft would not bounce away from the system. Similarly, the deployment velocities from a mothership stationed outside the orbit of the satellite can also be computed.

The functionality and reliability of these trajectories is next discussed by generating landing conditions for a specific coefficient of restitution and modelling navigation and deployment errors. The covariance matrices for a global set of landing conditions can then be propagated to the surface and the most robust landing locations are identified.

The remaining of the paper is organized through the following sections: Section 2 describes the motivation and state-of-the-art of asteroid landing; Section 3 very briefly describes the methodology of the deterministic approach to design landing trajectories; Section 4 introduces the guidance, navigation and control

challenges for landing operations of passive systems; and finally Section 5 provides some conclusions.

2. State-of-the-art

In so far, a total of eight spacecraft have flown to, or by, twelve asteroids. However, hundreds of asteroids will need to be visited, if we are to fully understand the workings of our Solar System; particularly, its compositional diversity. Even more limited is the number of surface probes that have touched down on an asteroid or comet surface. Two landers have so far attempted to touchdown with limited success: MINERVA¹ and Philae². While instead three main spacecraft have performed similar landing operations; Hayabusa³, NEAR-Shoemaker⁴ and Rosetta⁵. Although, only Hayabusa attempted such a manoeuvre before the end of mission phase.

Landing on a small body, such as an asteroid or comet, substantially differs from landing on a deeper gravity well, such as that of Mars or the Moon. The extremely weak gravitational environment found in small bodies makes purely ballistic descent trajectories a viable option, since the touchdown velocities can be safely managed by the landing gear. All the aforementioned landings have in fact attempted ballistic descents. However, the same weak gravitational environment entails a completely different challenge: Unless sufficient energy is damped at touchdown, the lander may well bounce away of the asteroid, or bounce into a badly illuminated conditions, which may seriously jeopardize the mission⁶.

Particularly, this paper focuses on landing opportunities for binary asteroids. These are systems of two asteroids orbiting around their common centre of mass⁷. The only visited binary asteroid so far is Ida-Dactyl⁸, which was flown by Galileo spacecraft at 12.4 km/s, on the 26th August 1993, with a close approach of ~2400 km⁹.

The planetary science community has however a real interest in returning to a binary, particularly with a rendezvous mission. Such a mission would clearly contribute to settle the debate on the formation of these systems. Moreover, the poles of the larger asteroid (i.e. the primary thereafter) are likely to feature fresh material¹⁰, and thus unweathered and pristine. Hence, missions have been proposed and studied; such as MarcoPolo-R¹¹ and BASIX¹². Apart from their fascinating geological and geophysical history, binary asteroids offer also the opportunity to investigate the effectiveness of future asteroid deflection techniques: The NASA/ESA co-operative AIDA mission was intended to impact the small asteroid (i.e. the secondary thereafter) in the binary asteroid Didymos, in order to test the kinetic impact deflection technique¹³.

AIDA consisted of two distinct spacecraft; NASA's DART (Double Asteroid Redirection Test), which is to impact the Didymos' secondary and ESA's Asteroid

Impact Mission (AIM), which was to rendezvous with Didymos to observe DART's impact. The AIM proposal included a small MASCOT-2 lander, of about 12 kg, as well as two 3U CubeSats to be deployed in the neighbourhood of Didymos. Even if AIM's future appears unlikely, since 2016 ESA Ministerial, the examples above indicate a clear interest to land small unpowered payloads into the surface of a binary system.

However, navigating within a binary asteroid system poses serious challenges, due to its highly perturbed dynamics and its natural satellite. Therefore, it might not be the best solution to put a mothership at risk by getting it into the vicinity of the binary in order to deploy an unpowered lander. The natural dynamics in binary asteroids could instead be exploited to achieve ballistic landing from a safe distance.

Ballistic landing on binary asteroids by means of natural manifold trajectories were studied by Tardivel and Scheeres¹⁴. A follow up work also discussed this strategy within the context of the deployment of a light lander as an optional payload for MarcoPolo-R mission¹⁵, including an statistical analysis of uncertainties for deployments near the L2 point. A similar L2 release strategy is depicted in Ferrari and Lavagna¹⁶. The consequent motion of the lander on the asteroid surface, after the initial touchdown, has also been investigated by several studies¹⁷⁻¹⁹.

This paper particularly focuses on searching landing opportunities for soft local-vertical touchdown in a binary asteroid. Landing trajectories are reverse engineered from the surface of both objects (i.e. primary and secondary), by propagating the model backwards in time. A dense grid of latitude-longitude nodes, homogeneously distributed over the entire surface of both objects, allows us to obtain a global map of feasible descend opportunities for unpowered landers.

3. A Global Map of Landing Opportunities

The mission architecture considered in this paper is that of a mothership which carries one (or several) landers. Once the mothership reaches the binary system, it would start orbiting near the binary and perform the necessary science operations. The mothership should be sufficiently close to the binary system to perform satisfactorily detailed observations; however, it should also remain sufficiently far away from the system's barycentre to prevent any collision risk or potential contamination of instruments and sensors.

The following section will briefly summarize the asteroid model and dynamical framework used. Then, Section 3.2 provides a general description of the methodology used to map the local vertical landing conditions over the entire surface of the binary. Section 3.3 will discuss some of the results. For further detail and/or discussion, the reader is referred to Celik and Sanchez²⁰.

3.1 Asteroid Model and Dynamical Framework

Binary asteroids are considered here as being of spherical shape and of constant density; both primary and secondary objects. Whereas all the secondaries that have been observed are somewhat elongated, primaries feature an approximately spherical shape²¹⁻²³. Nevertheless, a spherical shape provides a reasonable representation, which captures well the main underlying features of the dynamics of the full three body problem. Besides, the methodology described in Section 3.2 would also be applicable to higher fidelity shape models.

Hence, the Circular Restricted Three Body Problem (CR3BP) is used as a dynamical framework to estimate the motion of a massless spacecraft near the two asteroids. Thus, in a synodic reference frame centred in the barycentre of the binary system, the unpropelled motion of the landing spacecraft can be modelled by^{24,25} with the usual normalized set of ordinary differential equations:

$$\begin{aligned}\ddot{x} &= 2\dot{y} + \frac{\partial\Omega}{\partial x} \\ \ddot{y} &= -2\dot{x} + \frac{\partial\Omega}{\partial y} \\ \ddot{z} &= \frac{\partial\Omega}{\partial z}\end{aligned}\quad (1)$$

where the potential function Ω is defined as:

$$\Omega = \frac{x^2 + y^2}{2} + \frac{1-\mu}{r_p} + \frac{\mu}{r_s} \quad (2)$$

where r_p and r_s are the distances to the primary and secondary respectively. The mass parameter μ can be conveniently defined as:

$$\mu = \frac{n^3}{n^3 + 1} \quad (3)$$

where n is the secondary-to-primary radius ratio of the specific binary we want to model²⁰.

The mechanical energy in the CR3BP is represented by the Jacobi Constant C :

$$C = 2U - V^2 \quad (4)$$

where V is the spacecraft speed given in rotating frame of reference.

For a given set of initial conditions, the Jacobi Constant defines the accessible and forbidden zones of motion. From the expression in Eq.(4), it can be deduced that there are locations, for which at some energies, the velocity of the motion may become an imaginary number, which clearly indicates the physical impossibility of motion within those locations at those energy levels. Hence, zero-velocity surfaces (ZVS) are defined when one considers the condition $V=0$. ZVS shows which regions are accessible to motion at a given energy.

Figure 1 depicts a scenario on which the mothership is flying on a sufficiently high Jacobi Constant such that motion can only occur around the primary, the secondary or in a region exterior to the whole binary system. Such an operational orbit would be ideal for the safety of the mothership, since transitions between these three regions of allowed motion cannot occur as there are no connections between them. Thus, the mothership cannot possibly collide with the asteroid.

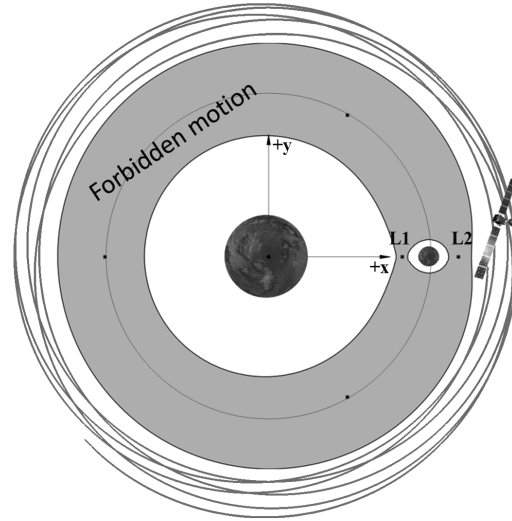


Figure 1. Illustration of mission architecture

3.2 Methodology

According to the scenario depicted in Figure 1, the deployment must be performed such that the lander is provided with sufficient energy for the ZVS to open at the L2 point, and a transition may thus occur. It is envisaged that the mothership is equipped with a simple spring mechanism capable to deploy the lander at most at 2 m/s²⁶.

Once the scenario is defined, landing trajectories are now in fact reverse engineered, by defining the point in the surface where we want to land, and propagating backwards until some satisfactory deployment condition is found. Note that once the landing site is defined, only one design parameter requires to be determined, since local vertical direction is assumed, and this is the touchdown speed v_l .

In backward propagation, a touchdown speed v_l such that its Jacobi Constant is equal to the L2 point $v_l(C_{L2})$ would be ensured not to reach the exterior region, where the mothership lingers. On the other hand, a touchdown speed $v_l \gg v_l(C_{L2})$ will instead easily reach the exterior region. A bisection search algorithm is then used to iterate between these two limits, until a minimum velocity is found that reaches the orbital altitude where the mothership may be encountered.

3.3 Results

A key requirement for landing opportunities is to allow for the slowest possible touchdown speed; firstly, to prevent damage to the spacecraft and its payload and, secondly, to minimize the risk of bouncing off the system if sufficient damping of the energy at touchdown is not achieved.

Table 1. The properties of notional average binary asteroid²⁰.

	Primary	Secondary
Diameter [m]	1000	250
Density [kg/m ³]	1700	
Mass [kg]	8.9×10^{11}	1.4×10^{10}
Orbit semi-major axis [m]	1950	
Orbital period [h]	19.4 h	

Figure 2 summarises the results of the bisection search to find the minimum possible landing velocity. The results have been dimensionalized to represent an *average* binary system²⁰ such as that represented in Table 1.

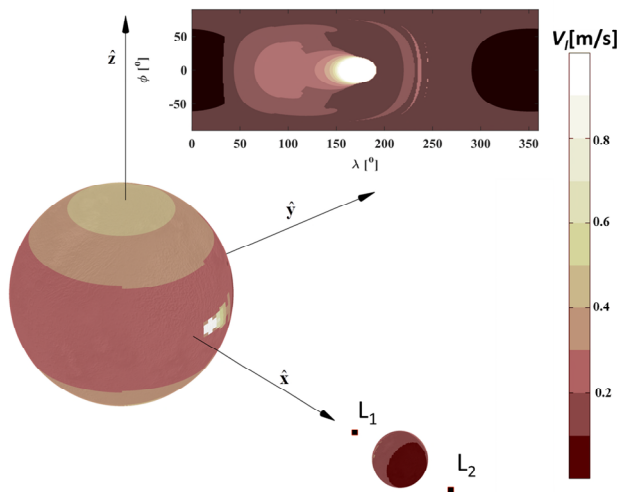


Figure 2. Minimum touchdown speed for the binary system in Table 1. Landing speed for the Secondary object is also represented in a Mercator projection in the top part of the figure.

As shown in Figure 2, the primary occupies the lowest part of the gravity well of the binary. Thus, as expected, the ballistic descent trajectories touchdown at higher velocities than at the secondary. Most of the surface of the secondary is instead reachable with touchdown velocities near 10 cm/s. It is noteworthy that most of the secondary surface is accessible at touchdown velocities lower than the two-body escape velocity, approximately 35 cm/sec in this case.

Figure 3 shows several examples of landing trajectories, both plotted in the synodic reference frame of the dynamical framework used, and also in the

inertial reference frame. Thus, for example, we see how the secondary landing at latitude ϕ and longitude λ of 0 degrees is clearly influence by the dynamics near the L2 libration point. This, however, represents a nearly circular orbit that moves parallelly with the secondary, as seen in the inertial reference frame.

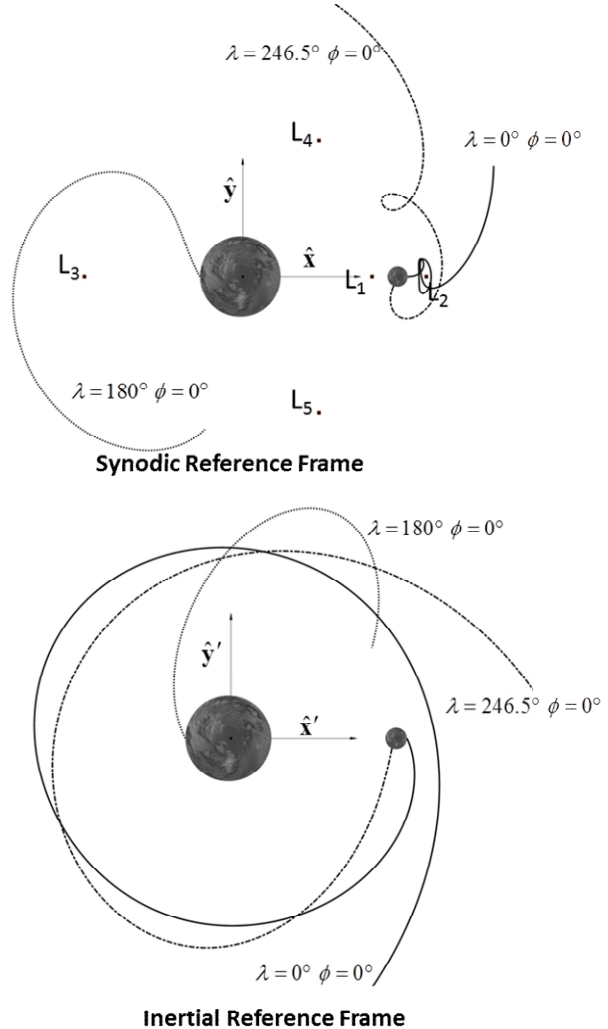


Figure 3. Landing trajectory for three locations within the binary, as seen in the synodic reference frame and the inertial reference frame.

Note that the secondary is assumed to be tidally locked²¹, hence, its attitude can be assumed fixed in the synodic reference frame, and the body's prime meridian ($\lambda=0$) can be arbitrarily defined as on the x-axis and on the far side of the system (facing the classical L2 point). However, the primary will have a fast rotation, which is likely to be near the point at which a body with negligible cohesion starts shedding mass²¹. The notional average binary used here assumes that the rotation of the primary is 2.2h, as well as a rotational axis is also perpendicular to the orbital plane of the secondary²¹.

Once the minimum velocities have been computed, the coefficient of restitution, or energy damping, required for these landing conditions to settle onto the surface of the asteroid, can be identified. This paper considers a simple model for the interaction of the spacecraft with the asteroid's surface; that of a bouncing ball with a specified coefficient of restitution $\varepsilon^{20,27}$.

The touchdown conditions can be described in local-vertical (LV) components as:

$$\mathbf{v}_{LV}^- = (\hat{\mathbf{n}} \cdot \mathbf{v}) \hat{\mathbf{n}} = v_l \hat{\mathbf{n}} \quad (5)$$

where the vector $\hat{\mathbf{n}}$ corresponds to the normal to the surface at the contact point, and the superscript (-) refers to the conditions just an infinitesimal instant before the rebound. Considering an impulsive rebound at touchdown with some loss of energy due to, for example, the deformation of the surface and/or spacecraft, the velocity conditions an infinitesimal instant after the rebound can be approximated as:

$$\mathbf{v}_{LV}^+ = -\varepsilon v_l \hat{\mathbf{n}} \quad (6)$$

where the coefficient of restitution ε defines the dissipation of energy.

Figure 4 summarises the values of the coefficient of restitution ε that ensures a sufficient condition to remain permanently in the neighbourhood of the body where the landing has been attempted. This sufficient condition is computed by estimating a coefficient of restitution $\varepsilon_{L1Close} = \mathbf{v}_{LVC1}^+ / \mathbf{v}_{LV}^-$, where \mathbf{v}_{LVC1}^+ represents the local vertical velocity after touchdown such that the Jacobi constant of the bouncing trajectory is that of the L1 equilibrium. This energy limit after the first bounce is chosen so that no escape can possibly occur from the neighbourhood of the asteroid, since zero velocity surfaces will be closed both at L1 and L2 points.

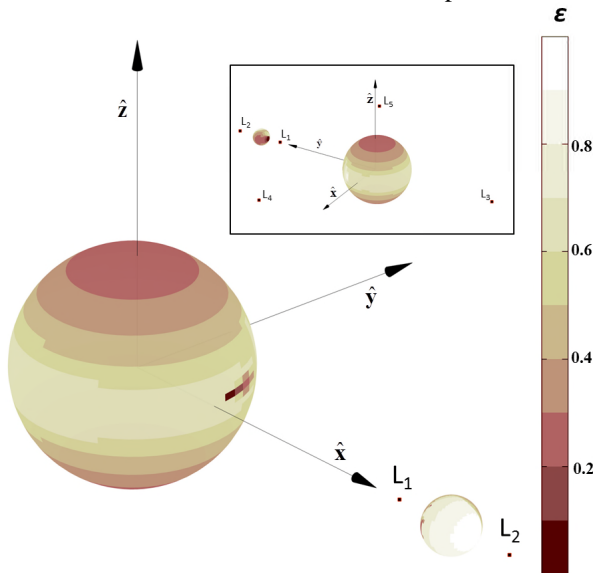


Figure 4. Required coefficient of restitution ε to ensure ZVS closed at L1 and L2 points.

Figure 4 provides important insights into the feasibility of the ballistic landing in a binary system. It shall be noted that Hayabusa and Philae's touchdown measured coefficients of restitution of $\varepsilon < 0.85^{2,3}$. Hence, considering the available data from past missions, it is clear that if assuming a conservative estimate for the coefficients of restitution ($\varepsilon \sim 0.9$), only the far side of the secondary would be available for landing. However, appropriate structural design may well allow for coefficients of restitution ε near $\sim 0.6^{28}$. At ε slightly lower than 0.7, large equatorial regions in the primary become available as landing locations.

Philae landing at comet 67P² observed coefficients of restitution $\varepsilon \approx 0.7$ in multiple bounces. Thus, the remaining of the paper will assume as unfeasible regions for landing any location where the coefficients of restitution ε in Figure 4 is below this limit. The primary is thus discarded and we will focus on the secondary as a landing location. Nevertheless, as shown in Celik and Sanchez²⁰, the results in Figure 4 are likely to be only worst case estimates of the necessary coefficient of restitution, since multiple bounces are likely to occur, and thus multiple opportunities energy damping before the spacecraft may definitely escape the system.

3.4 Deployment

Let us now focus on the deployment operation. The mothership is likely to release the landing system while in a trajectory taking it near to the binary, but yet safe according to the ZVS discussion in section 3.1. Thus, we assume that the release trajectory has a periapsis at the deployment point, and apoapsis near the sphere of influence of the binary system (SOI). At the deployment point the mothership shall have a normalized velocity

\mathbf{v}_{sc} :

$$\mathbf{v}_{sc} = \left(\sqrt{\frac{2}{r_{release}} - \frac{2}{r_{release} + r_{SOI}}} - r_{release} \right) \hat{\boldsymbol{\theta}}$$

where $\hat{\boldsymbol{\theta}} = \hat{\mathbf{h}} \times \hat{\mathbf{r}}$, $\hat{\mathbf{r}}$ is the release position unit radius vector and $\hat{\mathbf{h}}$ is the direction of the ballistic descent trajectory momentum vector. The initial state vector of the ballistic descent $[\mathbf{r}_{release} \quad \mathbf{v}_{release}]$ was computed with the aforementioned bisection algorithm²⁰. Note that the state vector $[\mathbf{r}_{release} \quad \mathbf{v}_{release}]$ is chosen such that two constraints are satisfied:

- The duration of the descent trajectory must be less than 12-h.
- The distance to the barycenter of the binary must be larger than 2340 meters.

The latter constrain ensures that the minimum distance to the secondary is 1.25 larger than the distance to the L2 point.

The deployment spring mechanism in the mothership must then provide an impulse such as:

$$\mathbf{v}_{spring} = \mathbf{v}_{release} - \mathbf{v}_{sc}.$$

Note that, ignoring navigation errors, the release location $\mathbf{r}_{release}$ is assumed to coincide with the position of the mothership at the release time \mathbf{r}_{sc} .

According the above deployment model, a relatively reduced region of the secondary is available for landing at coefficient of restitution $\epsilon > 0.7$. This region is depicted in Figure 5. It can be noted that some regions in the far side are no longer reachable, due to the fact that the ballistic descent trajectory takes more than 12 hours for those locations. This however could be solved by allowing touchdown velocities larger than the absolute minimum touchdown velocity (Figure 2), as will be seen later.

The homogeneous color in the Mercator projector indicates that any possible landing location requires a deployment velocity smaller than 20 cm/s, with a minimum deployment velocity of ~ 2 cm/s. Note that the deployment mechanism of Rosetta spacecraft was capable of providing a separation speed between 5 – 50 cm/s²⁹. More relevant to these results, AIM's deployment mechanism was being designed to provide 2-5 cm/s within ± 1 cm/s accuracy³⁰.

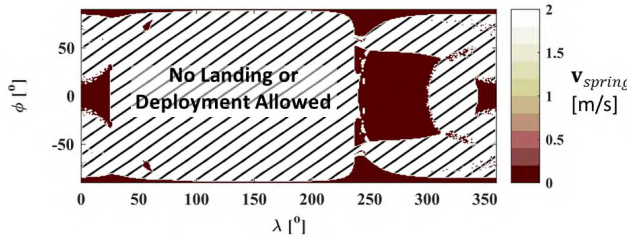


Figure 5. Deployment velocity as a function of location in the surface of the Secondary.

4. GNC Challenges

The purely deterministic analysis shown in the previous section demonstrated that ballistic descent trajectories are certainly possible in large regions of the secondary and possible for the primary. Although for the primary, a landing system capable to ensure sufficient energy damping at touchdown may be necessary.

However, inherent to the benefits and advantages of low energy trajectories also come their instabilities³¹. Moreover, the deployment will also be affected by inaccuracies of the knowledge of the state vector of the mothership, as well as by errors during the deployment caused by the deployment mechanism.

Many other sources of error and perturbations exist; such as the mass distribution of the asteroid. This paper, however, focuses now only on GNC related inaccuracies and their effect on the trajectories of the lander. Previous work by the authors also considered the variability of the asteroid's density, and it was shown to have a limited effect³². Finally, the fact that spherical shape is assumed may not necessarily be considered as a source of error; since if the shape of the asteroid was known, the same strategy could be used to compute new ballistic landing opportunities.

4.1 Deployment operation and errors

The navigation model will assume that both position \mathbf{r}_{sc} and velocity \mathbf{v}_{sc} of the mothership will be affected by navigation errors, and that the deployment velocity \mathbf{v}_{spring} may also be affected due to inaccuracies of the deployment mechanism. Table 2 summarizes the errors in position and velocity caused by the GNC and spring mechanism.

Table 2. Uncertainty and Error Sources

	3σ value
GNC position accuracy	± 30 m
GNC velocity accuracy	± 3 cm/s
Spring magnitude error	$\pm 30\%$
Spring angle error	$\pm 15^\circ$

Table 2 can be translated into a diagonal covariance matrix Q such as:

$$Q = \begin{pmatrix} \sigma_x^2 & 0 & 0 & 0 & 0 & 0 \\ 0 & \sigma_y^2 & 0 & 0 & 0 & 0 \\ 0 & 0 & \sigma_z^2 & 0 & 0 & 0 \\ \hline 0 & 0 & 0 & \sigma_{v_x}^2 & 0 & 0 \\ 0 & 0 & 0 & 0 & \sigma_{v_y}^2 & 0 \\ 0 & 0 & 0 & 0 & 0 & \sigma_{v_z}^2 \end{pmatrix}$$

where the diagonal contain the square root of the standard deviation for each component of the state vector. Q can then be propagated to the asteroid surface by means of the transition matrix Φ of the landing reference trajectory. The covariance matrix at the landing time $Q(t_l)$ can thus be computed as:

$$Q(t_l) = \Phi(t_l, t_d) Q(t_d) \Phi^T(t_l, t_d)$$

where the subscripts l and d denote landing and deployment times, respectively.

The covariance matrix at the landing time $Q(t_l)$ provides a linear approximation of the sensitivity of the landing trajectory to errors in GNC and deployment. The position errors in $Q(t_l)$ are represented within the first 3x3 submatrix of $Q(t_l)$:

$$Q(t_l) = \left(\begin{array}{ccc|cc} Q'_{xx} & Q'_{xy} & Q'_{xz} & & \\ Q'_{yx} & Q'_{yy} & Q'_{yz} & \mathbf{Q}_{TR} & \\ Q'_{zx} & Q'_{zy} & Q'_{zz} & & \\ \hline & \mathbf{Q}_{BL} & & & \mathbf{Q}_{BR} \end{array} \right)$$

However, the position errors will be best represented in a topocentric reference frame using the principal axis, in such a way that the previous top left matrix can be represented in its diagonal form:

$$Q(t_l) = \begin{pmatrix} a^2 & 0 & 0 \\ 0 & b^2 & 0 \\ 0 & 0 & c^2 \end{pmatrix}$$

At this point, the semi-major and minor axis (a , b) represent the footprint of the 1-sigma Gaussian distribution of the deployment errors. Finally, this data can be best represented with a single figure of merit $A_{2\sigma}$ such as:

$$A_{2\sigma} = 4 \frac{ab}{r_s^2}$$

where r_s is the radius of the secondary.

$A_{2\sigma}$ represents the area of the 2-sigma distribution footprint in units of cross sectional area of the secondary. Thus, a 2-sigma distribution footprint $A_{2\sigma}$ equal to 1 would represent a footprint as large as the asteroid itself, thus indicating a highly unreliable deployment. One would thus ideally aim for deployments such that $A_{2\sigma} \ll 1$.

4.2 Landing at minimum possible touchdown velocity

Figure 6 summarizes the 2-sigma distribution footprint $A_{2\sigma}$ as a function of latitude ϕ and longitude λ over the surface of the secondary. The fact that only small regions feature values of $A_{2\sigma} < 1$ indicates that at the accuracies in navigation and deployment assumed in Table 2 minimum touchdown velocity descent trajectories are not robust enough to provide a reliable landing.

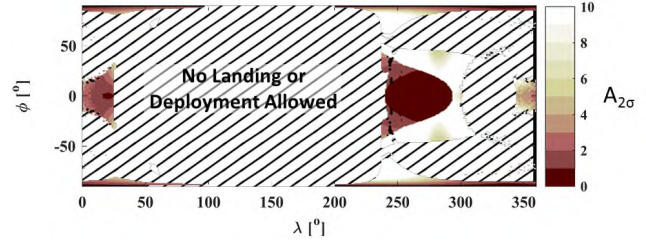


Figure 6. 2-sigma distribution footprint $A_{2\sigma}$ as a function of latitude ϕ and longitude λ over the surface of the secondary.

It follows then that landing trajectories with larger touchdown speed should be attempted. A larger than the minimum possible touchdown velocity implies a much faster descent trajectory, and thus shorter landing operations. Hence, initial errors in the descent trajectory may have less time to propagate, and thus may have a lesser impact on the descent trajectory. Nevertheless, note that the spring error is proportional to the velocity magnitude, and thus the latter statement requires to be demonstrated.

4.3 Landing at coefficients of restitution of 0.7

As discussed in section 3.3, a coefficient of restitution ϵ of 0.7 is defined as the minimum allowed restitution. Hence, landing operations that match precisely this coefficient of restitution are computed, as described in section 3.4. Figure 7 shows now the robustness of these descent trajectories to the same errors during the deployment described in Table 2. Note that the color scale has now changed since now most of the available landing space present values of $A_{2\sigma}$ below 1. Particularly, a relatively large region with $A_{2\sigma}$ in the range of [0.1, 0.2] extends longitudes from 310° to 25° and latitudes extending beyond 70° .

The minimum value of $A_{2\sigma}$ occurs at a longitude λ of 355° and the slightly off-equatorial latitude ϕ of 2° . The $A_{2\sigma}$ value at this location is of 0.114. A Monte Carlo analysis of this landing spot, with 10,000 randomly generated landing conditions, certifies that the probability of a first touchdown is of 100%. If we then assume a coefficient of restitution of 0.7 or lower, we can then be confident that the lander will remain in the surface of the secondary.

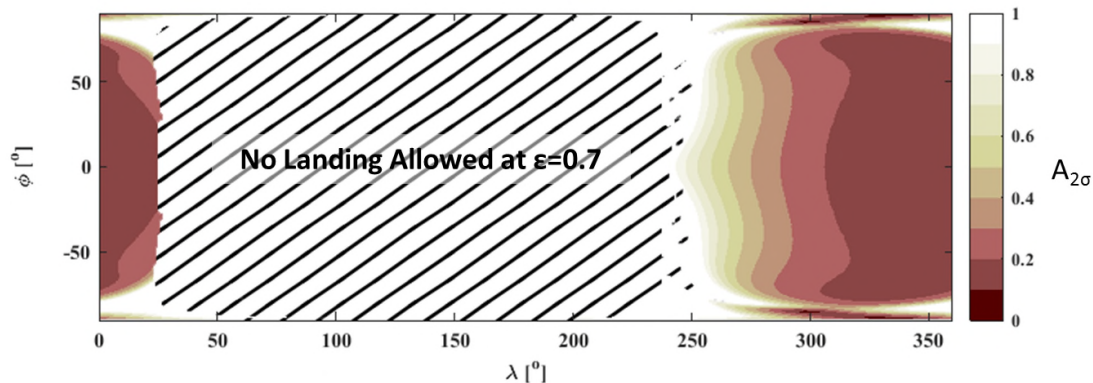


Figure 7. Adimensional Area of the 2-sigma ellipsoid of uncertainty of the landing state.

5. Conclusion

This paper has investigated the possibility to benefit from the natural dynamics near a binary asteroid as an efficient mean to deliver a lander, or scientific payload, onto its surface. The results show that landing at the primary requires some minimum landing system capable to damp excess of energy, to avoid bouncing out of the asteroid.

However, landing on the secondary seems compatible with completely passive systems, even if considering navigation and deployment errors in the order of 10 meters and 1 cm/s (1-sigma distribution). Near equatorial landing, in the region extending from 320° to 20° longitude, appear to be sufficiently robust to deployment errors.

Acknowledgements

Onur Celik is supported by Japanese Government Research Scholarship (Monbukagakusho) for his PhD research. Onur Celik also acknowledges the Royal Observatory of Belgium for providing the short-term research grant to carry out part of this study.

References

- 1 Yoshimitsu, T., Kubota, T. & Nakatani, I., "Operation of MINERVA rover in Hayabusa Asteroid Mission" in *AIAA 57th International Astronautical Congress, IAC 2006*. 1199-1209.
- 2 Biele, J. *et al.* The landing(s) of Philae and inferences about comet surface mechanical properties. *Science* **349**, doi:10.1126/science.aaa9816 (2015).
- 3 Yano, H. *et al.* Touchdown of the Hayabusa spacecraft at the Muses Sea on Itokawa. *Science* **312**, 1350-1353 (2006).
- 4 Veverka, J. *et al.* The landing of the NEAR-Shoemaker spacecraft on asteroid 433 Eros. *Nature* **413**, 390-393 (2001).
- 5 Accomazzo, A. *et al.* The final year of the Rosetta mission. *Acta Astronautica* **136**, 354-359,

doi:<https://doi.org/10.1016/j.actaastro.2017.03.027> (2017).

- 6 Ulamec, S. *et al.* Rosetta Lander - Philae: Operations on comet 67P/Churyumov-Gerasimenko, analysis of wake-up activities and final state. *Acta Astronautica* **137**, 38-43, doi:10.1016/j.actaastro.2017.04.005 (2017).
- 7 Margot, J. L. *et al.* Binary Asteroids in the Near-Earth Object Population. *Science* **296**, 1445-1448 (2002).
- 8 Belton, M. J. S. *et al.* The Discovery and Orbit of 1993 (243)1 Dactyl. *Icarus* **120**, 185-199, doi:<http://dx.doi.org/10.1006/icar.1996.0044> (1996).
- 9 Belton, M. J. S. *et al.* Galileo's Encounter with 243 Ida: An Overview of the Imaging Experiment. *Icarus* **120**, 1-19, doi:<http://dx.doi.org/10.1006/icar.1996.0032> (1996).
- 10 Walsh, K. J., Richardson, D. C. & Michel, P. Rotational breakup as the origin of small binary asteroids. *Nature* **454**, 188-191 (2008).
- 11 Michel, P. *et al.* MarcoPolo-R: Near-Earth Asteroid sample return mission selected for the assessment study phase of the ESA program cosmic vision. *Acta Astronautica* **93**, 530-538, doi:<http://dx.doi.org/10.1016/j.actaastro.2012.05.030> (2014).
- 12 Anderson, R. C., Scheeres, D., Chesley, S. & Team, B., "Binary asteroid in-situ explorer mission (basix): A mission concept to explore a binary near earth asteroid system" in *Lunar and Planetary Science Conference*. 1571.
- 13 Cheng, A. F. *et al.* Asteroid Impact and Deflection Assessment mission. *Acta Astronautica* **115**, 262-269, doi:<http://dx.doi.org/10.1016/j.actaastro.2015.05.021> (2015).
- 14 Tardivel, S. & Scheeres, D. J. Ballistic Deployment of Science Packages on Binary

- Asteroids. *Journal of Guidance, Control, and Dynamics* **36**, 700-709, doi:10.2514/1.59106 (2013).
- 15 Tardivel, S., Michel, P. & Scheeres, D. J. Deployment of a lander on the binary asteroid (175706) 1996 FG3, potential target of the european MarcoPolo-R sample return mission. *Acta Astronautica* **89**, 60-70 (2013).
 - 16 Ferrari, F. & Lavagna, M., "Asteroid impact mission: A possible approach to design effective close proximity operations to release mascot-2 lander" in *Proceedings of AIAA/AAS Astrodynamics Specialist Conference, Vail, CO, USA*.
 - 17 Tardivel, S., Canalias, E., Deleuze, M., Klesh, A. & Scheeres, D., "Landing MASCOT on Asteroid 1999 JU3: Solutions for Deploying Nanosats to Small-Body Surfaces" in *Lunar and Planetary Science Conference*. 1182.
 - 18 Sawai, S., Kawaguchi, J. i., Scheeres, D., Yoshizawa, N. & Ogasawara, M. Development of a target marker for landing on asteroids. *Journal of Spacecraft and Rockets* **38**, 601-608 (2001).
 - 19 Kubota, T., Sawai, S., Hashimoto, T. & Kawaguchi, J. i. Collision dynamics of a visual target marker for small-body exploration. *Advanced Robotics* **21**, 1635-1651 (2007).
 - 20 Celik, O. & Sánchez, J. P. Opportunities for Ballistic Soft Landing in Binary Asteroids. *Journal of Guidance, Control, and Dynamics* **40**, 1390-1402, doi:10.2514/1.G002181 (2017).
 - 21 Jacobson, S. A. & Scheeres, D. J. Dynamics of rotationally fissioned asteroids: Source of observed small asteroid systems. *Icarus* **214**, 161-178 (2011).
 - 22 Walsh, K. J. & Richardson, D. C. Binary near-Earth asteroid formation: Rubble pile model of tidal disruptions. *Icarus* **180**, 201-216 (2006).
 - 23 Ostro, S. J. *et al.* Radar imaging of binary near-Earth asteroid (66391) 1999 KW4. *Science* **314**, 1276-1280 (2006).
 - 24 Koon, W. S., Lo, M. W., Marsden, J. E. & Ross, S. D. *Dynamical systems, the three-body problem and space mission design*. (Marsden Books, 2008).
 - 25 Szebehely, V. *Theory of orbits*. (Academic Press, 1967).
 - 26 Lan, W. Poly picosatellite orbital deployer Mk III ICD. (California Polytechnic State University, San Luis Obispo, 2007).
 - 27 Greenwood, D. T. *Principles of dynamics*. 2nd ed. edn, (London: Prentice Hall., 1988).
 - 28 Ho, T., Biele, J. & Lange, C. AIM MASCOT-2 Asteroid Lander Concept Design Assessment Study. Technical Report. (German Aerospace Center (DLR), 2016).
 - 29 Ulamec, S. *et al.* Rosetta lander-landing and operations on comet 67P/Churyumov-Gerasimenko. *Acta Astronautica* **125**, 80-91 (2016).
 - 30 Walker, R., Binns, D., Carnelli, I., Kueppers, M. & Galvez, A., "CubeSat Opportunity Payload Intersatellite Network Sensors (COPINS) on the ESA Asteroid Impact Mission (AIM)" in *5th Interplanetary CubeSat Workshop (iCubeSat)*.
 - 31 Gómez, G., Jorba, A., Masdemont, J. & Simó, C. Study of the transfer from the Earth to a halo orbit around the equilibrium pointL 1. *Celestial Mechanics and Dynamical Astronomy* **56**, 541-562, doi:10.1007/BF00696185 (1993).
 - 32 Celik, O., Karatekin, O., Ritter, B. & Sánchez, J. P., "Reliability Analysis of Ballistic Landing in Binary Asteroid 65803 (1996 GT) Didymos under Uncertainty and GNC Error Considerations" in *26th International Symposium on Spaceflight Dynamics*.